Apolipoprotein E2 Accentuates Postprandial Inflammation and Diet-Induced Obesity to Promote Hyperinsulinemia in Mice

David G. Kuhel,[1] Eddy S. Konaniah,[1] Joshua E. Basford,[1] Courtney McVey,[1] Colleen T. Goodin,[1] Tapan K. Chatterjee,[2] Neal L. Weintraub,[2] and David Y. Hui[1]

Genetic studies have revealed the association between the ε2 allele of the apolipoprotein E (*apoE*) gene and greater risk of metabolic diseases. This study compared C57BL/6 mice in which the endogenous mouse gene has been replaced by the human *APOE2* or *APOE3* gene (*APOE2* and *APOE3* mice) to identify the mechanism underlying the relationship between ε2 and obesity and diabetes. In comparison with *APOE3* mice, the *APOE2* mice had elevated fasting plasma lipid and insulin levels and displayed prolonged postprandial hyperlipidemia accompanied by increased granulocyte number and inflammation 2 h after being fed a lipid-rich meal. In comparison with *APOE3* mice, the *APOE2* mice also showed increased adiposity when maintained on a Western-type, high-fat, high-cholesterol diet. Adipose tissue dysfunction with increased macrophage infiltration, abundant crown-like structures, and inflammation were also observed in adipose tissues of *APOE2* mice. The severe adipocyte dysfunction and tissue inflammation corresponded with the robust hyperinsulinemia observed in *APOE2* mice after being fed the Western-type diet. Taken together, these data showed that impaired plasma clearance of apoE2-containing, triglyceride-rich lipoproteins promotes lipid redistribution to neutrophils and adipocytes to accentuate inflammation and adiposity, thereby accelerating the development of hyperinsulinemia that will ultimately lead to advanced metabolic diseases. ***Diabetes* 62:382–391, 2013**

Apolipoprotein E (apoE) is a 34-kDa protein found in plasma associated with several classes of lipoproteins with a primary function in cholesterol and lipid transport (1). It is expressed in most cell types, including hepatocytes, smooth muscle, macrophages, adipocytes, and the central nervous system (1). In addition to facilitating lipid transport between various tissues and organs, apoE also has lipid transport–independent functions, such as the modulation of cell signaling, oxidation, and enzyme activation (2). Both lipid transport–dependent and –independent functions of apoE can modulate the progression and severity of a wide spectrum of metabolic diseases. The human *APOE* gene exists with three major polymorphic alleles. The most common allele, with a frequency of ~75%, is ε3, which imparts metabolic benefits due to the anti-inflammatory and antioxidative properties of apoE3. The ε4 allele, with a frequency of ~15%, encodes apoE4, which is proinflammatory and thus increases the risk for both cardiovascular disease and neurodegenerative disorders such as Alzheimer disease (1,2).

The relationship between the ε2 allele with metabolic disease risk is less clear. Typically, ε2 carriers have lower plasma cholesterol levels (3) but tend to have higher plasma triglyceride levels and are prone to developing type III dyslipoproteinemia (3,4), putting them at greater risk for metabolic-associated diseases. Although several independent studies have failed to identify an association between ε2 mutation and risk of type 2 diabetes (5–8), genetic studies in two other populations have revealed the association of the ε2 allele with higher BMI (odds ratio 3.55) and waist circumference (odds ratio 3.3) (4,9). A large-scale meta-analysis combining data from 30 independent studies showed that ε2 carriers have a moderately increased risk of developing type 2 diabetes (10). Diabetic ε2 carriers also have a twofold increased risk and severity of coronary artery disease compared with ε3 patients with diabetes (11,12). In nondiabetic patients, the ε2 allele is an independent risk factor for end-stage renal disease, peripheral vascular diseases such as cerebrovascular disease and ischemia of lower extremity arteries, and carotid atherosclerosis (13–16). The mechanism(s) underlying the contribution of apoE2 toward obesity, diabetes, and peripheral vascular disease has not been elucidated.

A well-established role of apoE is its ability to bind LDL receptor family proteins to mediate clearance of triglyceride-rich lipoproteins from circulation (1). ApoE2 is defective in binding to the LDL receptor (1). Although the majority of ε2 homozygotes have normal or even lower plasma cholesterol levels (1), almost all heterozygous and homozygous ε2 carriers have elevated triglyceride levels due to impaired hepatic clearance of triglyceride-rich lipoproteins, including the chylomicron remnants derived postprandially after a fatty meal (1,17). With increasing evidence suggesting that the postprandial increase of plasma triglyceride levels promotes systemic inflammation (18–23), which increases the risk of metabolic diseases (22,23), it is reasonable to postulate that the elevated metabolic disease risk associated with the ε2 allele may be due to sustained postprandial inflammation as a consequence of delayed postprandial triglyceride-rich lipoprotein clearance. To test this hypothesis, this study compared fatty meal–induced postprandial inflammation between mice in which the endogenous mouse *apoE* gene has been replaced by either the human *APOE2* or *APOE3* gene. The consequence of chronic high-fat feeding on tissue inflammation and obesity/diabetes development between *APOE2* and *APOE3* gene replacement mice was also explored.

From the [1]Department of Pathology, Metabolic Diseases Institute, University of Cincinnati College of Medicine, Cincinnati, Ohio; and the [2]Department of Internal Medicine, Division of Cardiovascular Diseases, University of Cincinnati College of Medicine, Cincinnati, Ohio.
Corresponding author: David Y. Hui, huidy@ucmail.uc.edu.
Received 28 March 2012 and accepted 17 July 2012.
DOI: 10.2337/db12-0390

RESEARCH DESIGN AND METHODS

Animals and diets. Gene replacement mice, in which the endogenous mouse *apoE* gene has been replaced at the same locus with the human *APOE2* or *APOE3* gene (24,25), hereafter designated as *APOE2* and *APOE3* mice, were purchased from Taconic (Hudson, NY), where they were back-crossed to C57BL/6 background through nine and eight generations, respectively. The human *APOE* genotypes in these animals were confirmed by restriction isotyping after gene amplification as previously described (26). The mice were fed either chow (Teklad, Madison, WI) or a Western-type, high-fat, high-cholesterol diet containing 21.2% fat and 0.2% cholesterol (TD88137; Teklad). Animals were maintained under controlled environmental conditions with free access to food and water. All animal protocols were approved by the University of Cincinnati Institutional Animal Use and Care Committee.

Weight and adiposity measurements. Age-matched *APOE2* and *APOE3* mice were housed according to their genotype with one to three mice per cage. Food consumption was monitored daily over a 1-week period. No obvious difference in the average amounts of food consumed per animal was observed regardless of housing conditions. Body weight and adiposity measurements were performed every 2 weeks. Weights were obtained using a Denver 300 K scale. Adiposity measurements were obtained using an EchoMRI Whole-Body Composition Analyzer (Echo Medical Systems, Houston, TX), as described previously (27).

Blood chemistry. Blood was collected from mice after an overnight fast. Blood glucose was determined with an Accu-Chek Active Glucometer (Roche Applied Science, Indianapolis, IN). Plasma insulin levels were measured with the Ultra Sensitive Rat Insulin ELISA kit (Crystal Chem, Chicago, IL). Plasma adiponectin levels were measured by mouse Adiponectin/Acrp30 DuoSet ELISA (R&D Systems, Minneapolis, MN). Plasma levels of leptin and other cytokines were determined using MILLIPLEX MAP Mouse Adipokine Panel (Millipore, St. Charles, MO). Plasma cholesterol and triglycerides were determined using Infinity cholesterol and triglyceride kits (Thermo Fisher Scientific, Middletown, NJ). Samples from each mouse were analyzed individually except for lipoprotein separation, in which two separately pooled samples, each with 0.25 mL plasma from three animals in each group, were subjected to fast-performance liquid chromatography (FPLC) gel filtration on two Superose 6 columns connected in series. Individual fractions in the FPLC were analyzed based on cholesterol content and by Western blot analysis with goat anti-human apoB (Millipore) and rabbit anti-human apoE (Dako) antibodies at 1:5,000 dilutions, as described previously (28).

Postprandial lipid clearance. Mice were fasted overnight and then fed a bolus lipid-rich meal (15 μL olive oil and 0.2 μCi [^{14}C]triolein per gram body weight) by stomach gavage. Blood (50 μL) was obtained from the tail vein before and 15, 30, 60, 120, and 180 min afterward. Plasma was obtained after centrifugation and used to measure triglyceride levels and determine radioactivity by liquid scintillation counting.

Glucose tolerance and insulin sensitivity tests. A glucose solution was administered orally by stomach gavage to chow-fed *APOE2* and *APOE3* mice (2 g/kg body weight) after an overnight fast. Insulin sensitivity was monitored by intraperitoneal injection of 0.75 units pig insulin per gram body weight after a 10-h fast. Blood was obtained from the tail vein before and every 15 min after glucose or insulin administration to measure glucose levels.

Adipose tissue histology. Subcutaneous (inguinal) and visceral (gonadal) adipose tissues were fixed in isotonic neutral 4% paraformaldehyde solutions prior to embedding in paraffin. Three 5-μm sections from different levels of each depot obtained from each mouse (four *APOE2* and six *APOE3* mice) were analyzed for adipocyte size and crown-like structures after staining with hematoxylin and eosin. Adipocyte sizes were determined as adipocyte area of 480 random adipocytes. Crown-like structures, indicative of inflammatory macrophages surrounding dead adipocytes (29), were identified based on aggregates of nucleated cells surrounding individual adipocytes. Crown-like structure density was obtained by counting the total number in each section compared with the total number of adipocytes.

RNA quantification. Total RNA was isolated with TRIzol reagent (Invitrogen) and treated with Turbo DNase (Applied Biosystems/Ambion, Austin, TX). cDNA was generated using the iScript cDNA Synthesis Kit (Bio-Rad Laboratories, Hercules, CA). Quantitative real-time PCR was performed on a StepOnePlus Fast Thermocycler using Fast SYBR Green Master Mix (Applied Biosystems, Carlsbad, CA) with primer sequences as shown in Table 1.

Flow cytometry. Flow cytometry analysis was performed on a Guava EasyCyte 8HT System and analyzed using Guava InCyte (Millipore, Hayward, CA). In brief, mice fasted overnight were given an oral gavage of 200 μL olive oil. Blood was collected from the submandibular vein in heparinized tubes before and 2 h after the gavage. Erythrocytes were lysed with RBC lysis buffer (eBioscience, San Diego, CA) for 10 min at room temperature twice and then washed once in flow cytometry staining buffer (FCSB; Ca^{2+}/Mg^{2+}-free Hanks' balanced salt solution with 0.3% NaN_3 and 1% BSA [fraction V; Sigma]). FCSB was used for all washes and antibody incubations unless otherwise indicated. All remaining incubations were carried out at 4°C. Nonspecific binding was blocked using CD16/32 antibody (eBioscience, San Diego, CA). Cells were washed and incubated for 45 min with various extracellular-labeling antibodies at 1:25 dilution and then fixed in 2% paraformaldehyde solution overnight. Cells were permeabilized with BD Cytofix/Cytoperm Plus Kit (BD Biosciences, Franklin Lakes, NJ), incubated with 1:25 dilutions of antibodies specific for intracellular markers, and subjected to flow cytometry analysis. Conjugated antibodies to nitric oxide synthase (NOS2), Lys6G, and CD11b were purchased from BD Biosciences. For neutral lipid staining, leukocytes were incubated with HCS LipidTOX (Invitrogen) at 1:100 for 1 h prior to flow cytometry analysis. The magnitude of lipid accumulation was determined based on green fluorescent intensity measured at 488-nm excitation and 518-nm emission. Adipose tissue macrophage content was assessed based on positive staining of stromal-vascular cells with F4/80 antibodies (eBioscience) after enzymatic tissue disaggregation with type I collagenase (Worthington, Lakewood, NJ).

Statistics. Statistical analyses were performed using Microsoft Excel spreadsheet or SigmaPlot version 11.0 software. Data are expressed as means ± SDs, except where noted in the figure legend. Differences were considered significant at $P < 0.05$ based on ANOVA analyses with Bonferroni post hoc test or Student *t* test.

RESULTS

Prolonged postprandial hypertriglyceridemia in *APOE2* mice. Male *APOE2* and *APOE3* mice were placed on either a basal rodent chow and/or fed a Western-type, high-fat, high-cholesterol diet beginning at 6 weeks of age. Fasting plasma lipid levels were determined after 4 weeks. Consistent with results reported previously (27,28), *APOE2* mice have significantly higher plasma triglyceride and cholesterol levels compared with the *APOE3* mice under both dietary conditions (Fig. 1*A* and *B*). Interestingly, plasma triglyceride levels in *APOE2* mice fed the basal diet were higher and their plasma cholesterol levels were similar to *APOE3* mice fed the Western-type diet. Hyperlipidemia was further exaggerated in *APOE2* mice after feeding the Western-type diet (Fig. 1*A* and *B*). When the mice maintained on basal diet were challenged with

TABLE 1
Primer sequences used for RT-PCR amplification of RNA

Gene	Sense primer	Antisense primer
Cyclophilin A	TCATGTGCCAGGGTGGTGAC	CCATTCAGTCTTGGCAGTGC
F4/80	TGTCTGACAATTGGGATCTGCCCT	ATACGTTCCGAGAGTGTTGTGGCA
MCP-1	CCTCCTCCACCACCATGCA	CCAGCCGGCAACTGTGA
MIP-1α	TTTGAAACCAGCAGCCTTTGCTCC	TCAGGCATTCAGTTCCAGGTCAGT
TNF-α	ATCCGCGACGTGGAACTG	ACCGCCTGGAGTTCTGGAA
Leptin	GCAGCACACGATGGAAGCACTTAT	TTGGGCAGACCCATCAATAGGATT
Adiponectin	GTTGCAAGCTCTCCTGTTCC	CCAAGAAGACCTGCATCTCC
Mannose receptor	TCCGGTTGGAACCAGTTCCTCAAT	GGCTGGCTGTGATAAATGCTTGCT
NOS2	TTCACCCAGTTGTGCATCGACCTA	TCCATGGTCACCTCCAACACAAGA

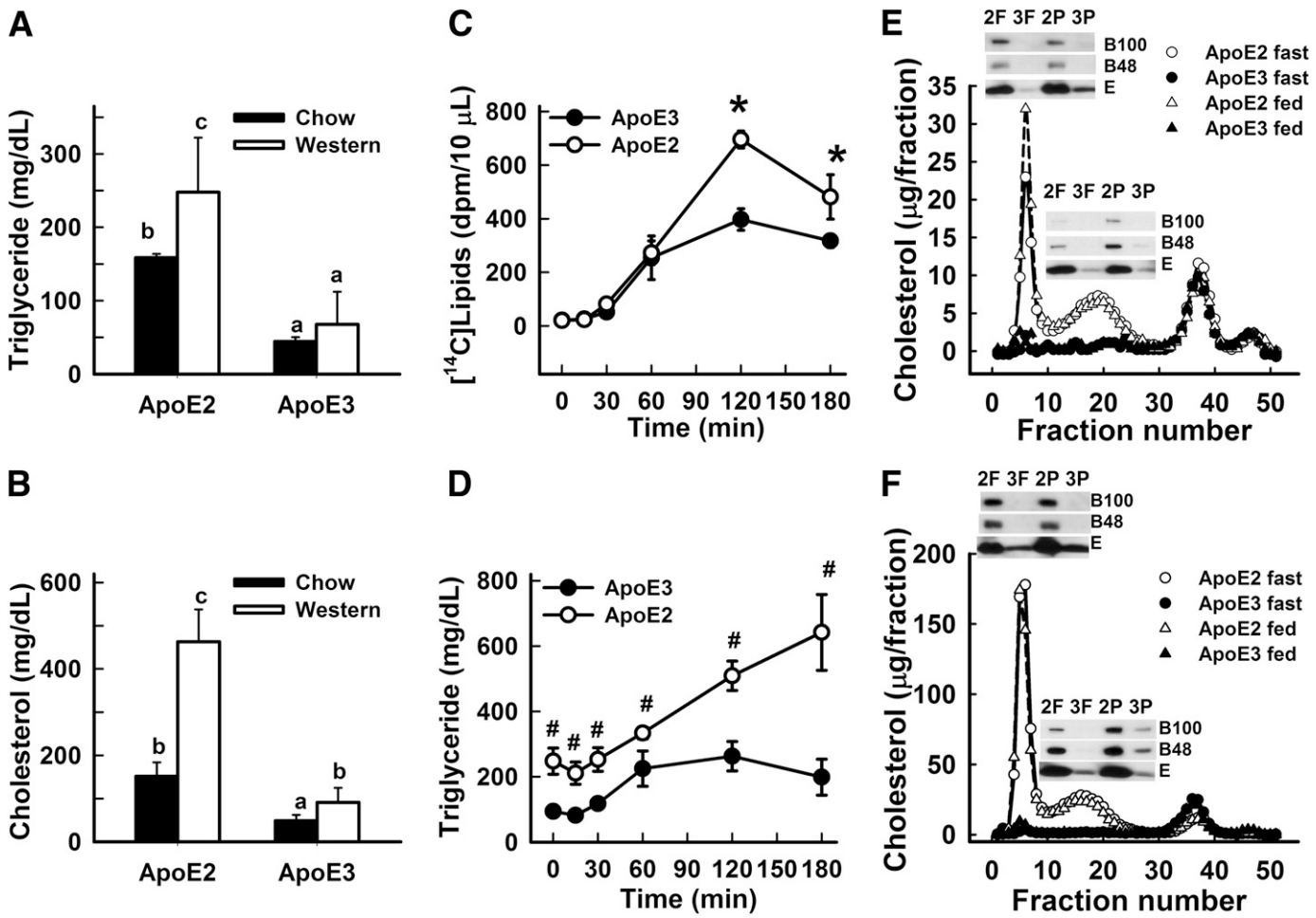

FIG. 1. Plasma lipid levels in *APOE2* and *APOE3* mice. *A*: Fasting triglyceride levels. *B*: Fasting cholesterol levels in *APOE2* and *APOE3* mice fed chow diet (filled bars) and after feeding the Western-type diet for 4 weeks (open bars). Bars with different letters were different at $P < 0.05$ ($n = 6$). *C*: Postprandial clearance of [^{14}C]lipids from plasma after feeding *APOE2* (open symbols) and *APOE3* (filled symbols) mice an olive oil meal containing [^{14}C]triolein. *D*: Postprandial plasma triglyceride levels in chow-fed *APOE2* (open symbols) and *APOE3* (filled symbols) 2 h after oral feeding a lipid-rich meal. The data in *C* and *D* represent mean ± SD from four mice in each group, with * and # indicating significant differences from the *APOE3* mice at $P < 0.05$ and $P < 0.01$, respectively. *E* and *F*: FPLC profiles from *APOE2* (open symbols) and *APOE3* mice (filled symbols) under both fasting (circle symbols) and postprandial (triangle symbols) conditions. The insets show Western blots of apoB100, apoB48, and apoE bands in VLDL (fractions 3–6) and IDL/LDL (fractions 18–21) of fasted (F) and postprandial (P) *APOE2* (2F and 2P) and *APOE3* (3F and 3P) mice. Note that the apoB proteins in *APOE3* mice were barely detectable by Western blots.

a bolus lipid-rich meal of olive oil containing [^{14}C]triolein, delayed plasma clearance of the radiolabeled lipids, indicative of defective triglyceride-rich lipoprotein clearance, was observed in *APOE2* mice (Fig. 1*C*). The impaired clearance of postprandial, triglyceride-rich lipoproteins resulted in robust postprandial hyperlipidemia in the *APOE2* mice (Fig. 1*D*). Analysis of lipoproteins in chow- and Western diet–fed mice under both fasting and postprandial conditions by FPLC revealed the accumulation of VLDL and LDL in the *APOE2* mice (Fig. 1*E* and *F*). Western blot analysis confirmed the accumulation of apoB100- and apoB48-containing lipoproteins with excess apoE in *APOE2* mice compared with *APOE3* mice (Fig. 1*E* and *F*). These results illustrated that *APOE2* mice recapitulated the abnormal lipoprotein metabolism in ε2 human subjects, and thus can be used to assess the influence of apoE2 on metabolic diseases.

Elevated postprandial inflammation in *APOE2* mice. Triglyceride-rich lipoproteins and postprandial lipidemia are major risk factors for metabolic and vascular diseases because of their direct influence on leukocyte activation, with increased neutrophil cell count and activation to exacerbate inflammation (19,20,30,31). Therefore, we also examined the role of the apoE2-associated delay in postprandial triglyceride-rich lipoprotein clearance on inflammation. Blood from chow-fed *APOE2* and *APOE3* mice was collected after an overnight fast and 2 h after a bolus olive oil meal for flow cytometry analysis. Whereas no differences in the number of granulocytes, monocytes, and lymphocytes were observed between *APOE2* and *APOE3* mice during the fasting state, the *APOE2* mice had a significantly higher number of granulocytes compared with *APOE3* mice during the postprandial period (Fig. 2*A*–*C*). Both *APOE2* and *APOE3* mice also exhibited reduced levels of monocytes in circulation postprandially, but no statistically significant differences were observed between *APOE2* and *APOE3* mice (Fig. 2*C*). Interestingly, a significant increase in neutral lipid accumulation in neutrophils was observed in *APOE2* mice compared with *APOE3* mice 2 h after a bolus lipid-rich meal (Fig. 2*D*–*F*). These observations indicate that delayed clearance of apoE2-containing, triglyceride-rich lipoproteins leads to their

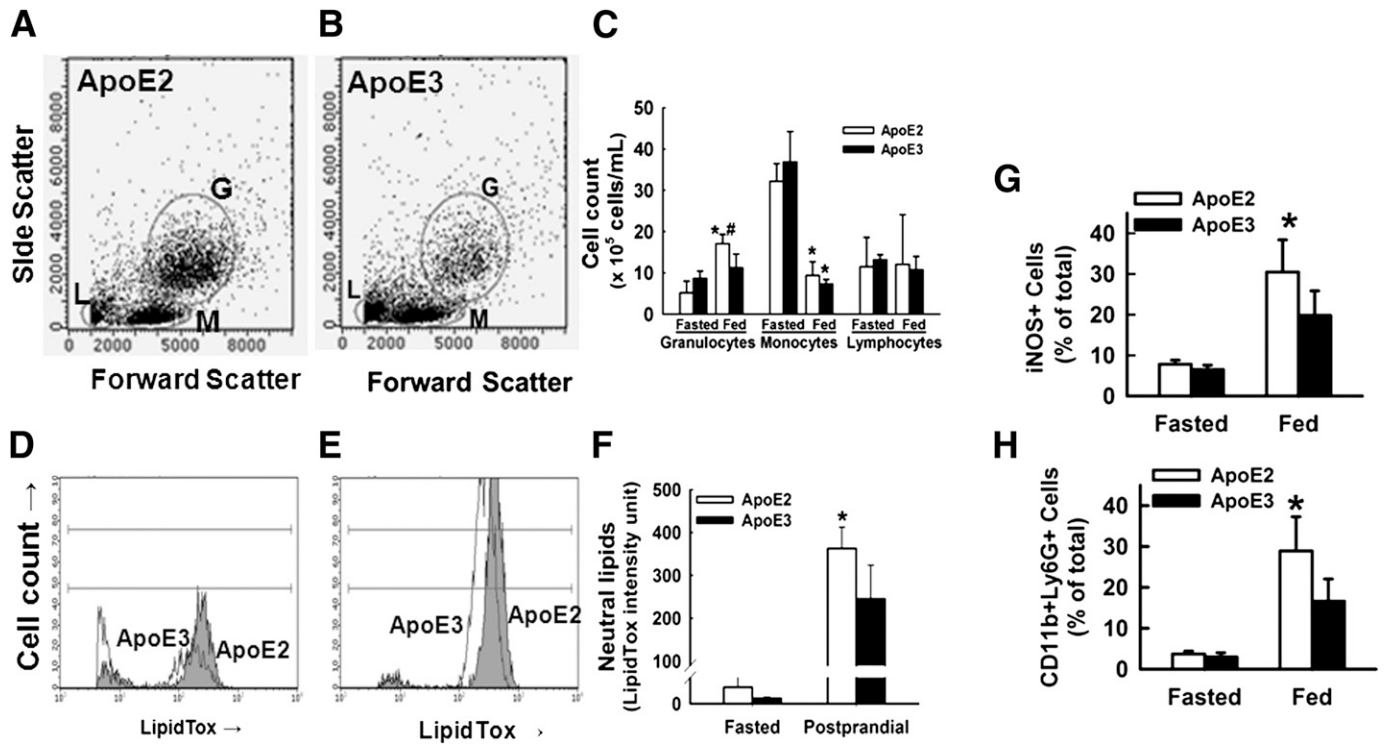

FIG. 2. Flow cytometry analysis of blood leukocytes in *APOE2* and *APOE3* mice. *A* and *B*: Representative plots of blood cells showing forward and side scattering of lymphocytes (L), monocytes (M), and granulocytes (G) from *APOE2* and *APOE3* mice, respectively, 2 h after feeding a lipid-rich meal. *C*: Bar graph showing the average number of each cell type ± SD in four *APOE2* (open bars) and six *APOE3* (filled bars) mice after overnight fast and 2 h after feeding a lipid-rich meal. *$P < 0.05$, difference from fasted mice of the same genotype; #$P < 0.05$, difference from *APOE3* mice under same treatment conditions ($n = 6$ in each group). *D* and *E*: Representative histogram of granulocytes after staining with the fluorescent neutral lipid stain LipidTox. *F*: Bar graph showing mean neutral lipid staining intensity ± SD from four *APOE2* (open bars) and eight *APOE3* (filled bars) mice before (fasted) and 2 h after lipid meal feeding (postprandial). *$P < 0.05$, difference from the *APOE3* mice. *G*: Inducible NOS (iNOS)–positive neutrophils. *H*: CD11b and Ly6G double-positive cells as the mean percentage of total leukocytes ± SD in the blood of four *APOE2* (open bars) and six *APOE3* (filled bars) mice before (fasted) or 2 h after feeding a lipid-rich meal (fed). *$P < 0.05$, difference from *APOE3* mice under same feeding conditions ($n = 6$).

elevated transport to granulocytes, a process that may promote systemic inflammation (19,20). Indeed, whereas fasting *APOE2* mice showed no differences in either $CD11b^+Ly6G^+$ granulocytes or granulocyte expression of inducible NOS2 compared with *APOE3* mice, significantly higher numbers of both $NOS2^+$ and $CD11b^+Ly6G^+$ granulocytes were observed in *APOE2* mice during the postprandial period compared with those observed in *APOE3* mice (Fig. 2*G* and *H*).

ApoE2 promotes diet-induced obesity and insulin resistance. The delay in postprandial triglyceride-rich lipoprotein clearance may also increase the partitioning of dietary fat to adipose tissues for storage. To test this possibility, we compared the body weights of *APOE2* and *APOE3* mice maintained on basal chow diet and then monitored their body weights in response to Western diet feeding. Results showed that 10-week-old male *APOE2* mice were slightly heavier than *APOE3* mice on chow diet (Fig. 3*A*). After Western diet feeding for 4 weeks, the *APOE2* mice gained significantly more weight compared with the *APOE3* mice (Fig. 3*A*). Analysis of body composition by nuclear magnetic resonance revealed that the differences in body weight gain between *APOE2* and *APOE3* mice were due to significantly higher body fat content in *APOE2* mice (Fig. 3*B*).

Fasting glucose levels were similar between *APOE2* and *APOE3* mice under basal dietary conditions. Both groups of mice showed a slight but statistically insignificant increase in fasting glucose levels, but their fasting insulin levels were significantly elevated after 4 weeks on Western-type diet (Fig. 4*A* and *B*). Interestingly, fasting insulin levels were higher in *APOE2* mice compared with *APOE3* mice under both dietary conditions. In fact, fasting insulin levels in chow-fed *APOE2* mice were similar to those observed in *APOE3* mice fed the Western-type diet for 4 weeks (Fig. 4*B*), and the Western diet further elevated fasting insulin levels in *APOE2* mice to levels approximately three times higher than those observed in Western diet–fed *APOE3* mice (Fig. 4*B*). Calculations of homeostasis model assessment of insulin resistance index suggested that *APOE2* mice are prediabetic with hyperinsulinemia even under basal dietary conditions (Fig. 4*C*). This hypothesis was confirmed by data showing a small but statistically significant increase of glucose intolerance in chow-fed *APOE2* mice after an oral glucose load (Fig. 4*D*), despite their elevated plasma insulin levels compared with *APOE3* mice (Fig. 4*B*). The insulin resistance phenotype of *APOE2* mice was further confirmed by insulin tolerance tests, showing their delayed glucose disposal after insulin injection compared with that observed in *APOE3* mice (Fig. 4*E*).

ApoE2 promotes adipocyte dysfunction and inflammation. The robust diet-induced obesity and hyperinsulinemia along with elevated postprandial systemic inflammation observed in the *APOE2* mice suggests their potential increased susceptibility to diet-induced adipocyte dysfunction and inflammation compared with *APOE3* mice. Therefore, subcutaneous (inguinal) and visceral (gonadal) fat depots

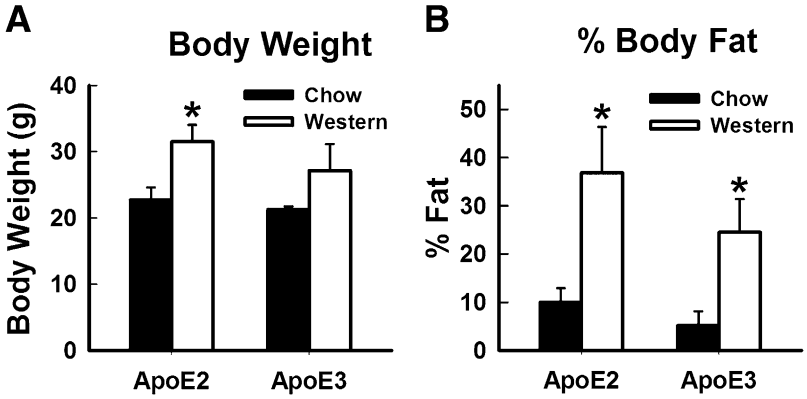

FIG. 3. Body weights and adiposity of *APOE2* and *APOE3* mice. Bar graphs showing mean body weights ± SD (*A*) and percent body fat ± SD (*B*) in 10-week-old male *APOE2* and *APOE3* mice fed either chow diet (filled bars) or 4 weeks after feeding the Western-type diet (open bars). *$P < 0.05$, difference from chow-fed mice ($n = 6$).

were harvested from *APOE2* and *APOE3* mice fed either basal or Western diet for 4 weeks for comparison. Histological examination of the adipose tissues revealed larger adipocytes in subcutaneous depots of *APOE2* mice compared with *APOE3* mice under chow-fed conditions (Fig. 5*A* and *B*). Significant enlargement of the adipocytes in both depots of *APOE2* and *APOE3* mice was observed after Western diet feeding, but the differences between *APOE2* and *APOE3* mice were no longer noticeable (Fig. 5*A* and *B*). The most striking difference between *APOE2* and *APOE3* mice was the prevalence of crown-like structures, indicative of dead adipocytes surrounded by macrophages (29), in the adipose tissues of *APOE2* mice (Fig. 5*C*). Although *APOE3* mice displayed a minimal, if any, number of crown-like structures in both subcutaneous and visceral adipose tissues under chow-fed conditions, and their presence was detectable only sporadically after 4 weeks of feeding with the Western-type diet, the crown-like structures were detectable consistently in both subcutaneous and visceral adipose depots of *APOE2* mice even when maintained under chow-fed conditions (Fig. 5*C*). The number of crown-like structures was further increased in both adipose depots of *APOE2* mice after Western diet feeding (Fig. 5*C*). The presence of crown-like structures, and their subsequent increase with Western diet feeding in

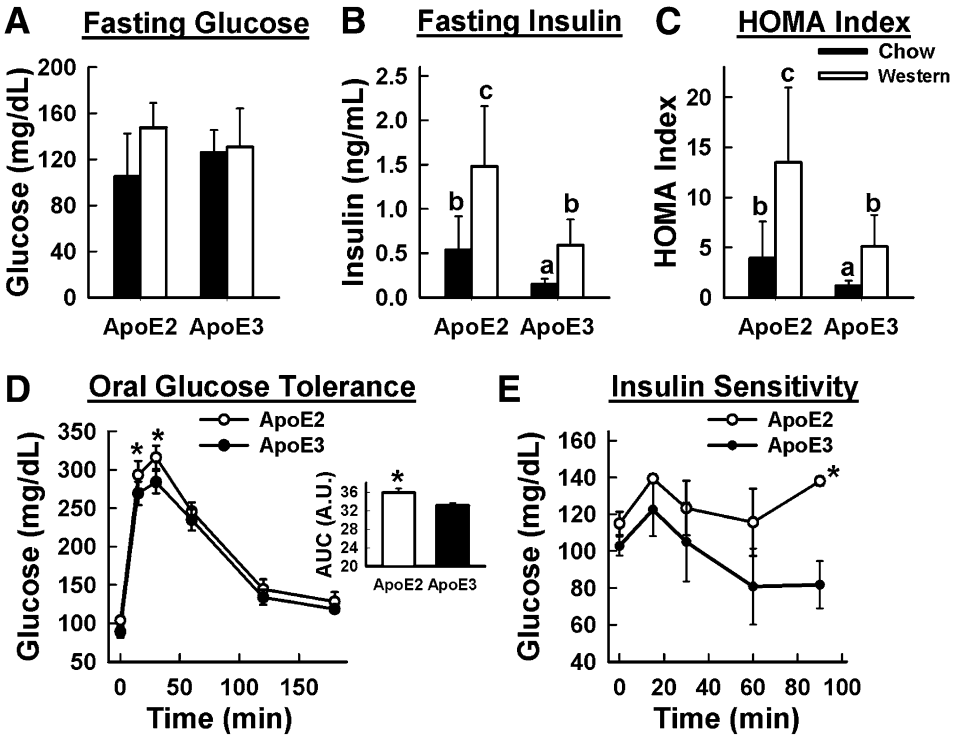

FIG. 4. Blood glucose and insulin levels. *A*: Mean fasting blood glucose ± SD. *B*: Fasting plasma insulin levels ± SD. *C*: Calculations of homeostasis model assessment of insulin resistance (HOMA) index in chow- (filled bars) and Western diet–fed (open bars) *APOE2* and *APOE3* mice. Bars with different letters denote significant differences at $P < 0.05$, whereas bars with similar letters were not statistically different ($n = 6$). Glucose tolerance tests with inset showing area under the curve (AUC) analysis (*D*) and insulin sensitivity tests (*E*) in *APOE2* (open symbols) and *APOE3* (filled symbols) mice. The data represent the mean from six mice in each group. *$P < 0.05$, difference from the *APOE3* mice. A.U., arbitrary units.

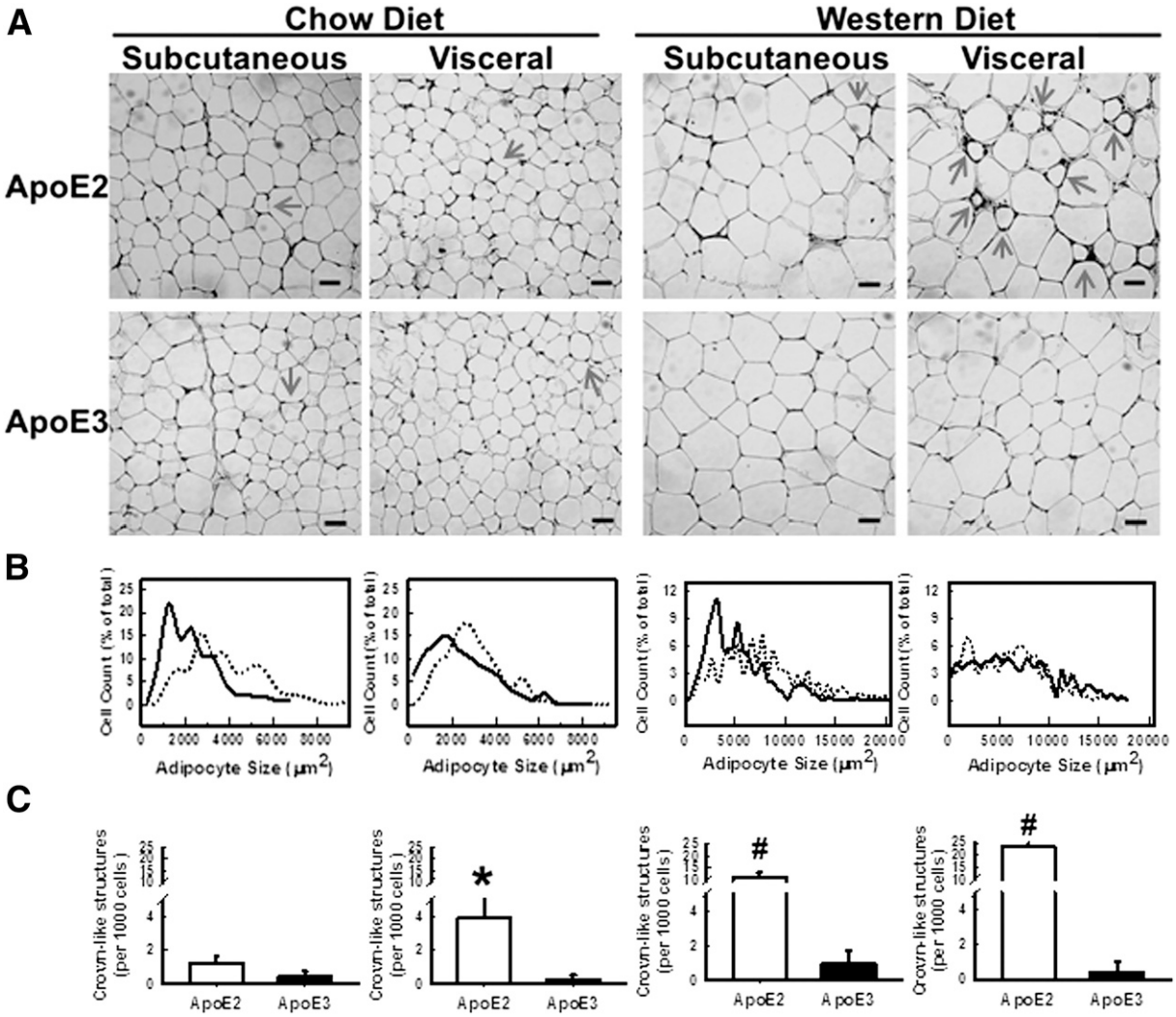

FIG. 5. Adipose tissue histology. *A*: Histological analysis of subcutaneous (inguinal) and visceral (gonadal) adipose tissues of *APOE2* and *APOE3* mice fed either chow diet or after feeding the Western diet for 4 weeks. Arrows point to representative crown-like structures in each image. Bars, 50 μm. *B*: Distribution of adipocyte cell sizes in subcutaneous (inguinal) and visceral (gonadal) adipose tissues of chow- and Western diet–fed *APOE2* (dotted lines) and *APOE3* (solid lines) mice. The data were obtained by measuring areas of 480 random adipocytes from three random fields from each mouse (n = 4 *APOE2* and 6 *APOE3* mice). *C*: Number of crown-like structures in subcutaneous and visceral adipose tissues of chow- and Western diet–fed *APOE2* (open bars) and *APOE3* (filled bars) mice. The data were obtained by counting the total number in each section compared with the total number of adipocytes and reported as mean ± SE. *P < 0.05, significant difference from the *APOE3* mice; #P < 0.01, significant difference from the *APOE3* mice.

adipose tissues of *APOE2* mice, is consistent with the interpretation that apoE2 promotes adipocyte dysfunction and increases susceptibility to diet-induced inflammation.

The analysis of adipokine expression revealed significantly elevated leptin expression in both subcutaneous and visceral adipose tissues after Western diet feeding (Fig. 6*A*). Consistent with results showing exaggerated diet-induced adiposity in *APOE2* mice, diet-induced leptin expression was also higher in the *APOE2* mice compared with *APOE3* mice (Fig. 6*A*). Interestingly, adiponectin expression levels were similar between chow- and Western diet–fed *APOE2* mice, whereas adiponectin expression levels in the subcutaneous tissue of *APOE3* mice were higher after Western diet feeding (Fig. 6*B*). As a result, adiponectin-to-leptin ratios in subcutaneous and visceral fat depots were lower in *APOE2* mice, and the differences were further exaggerated upon Western diet feeding. These data provided additional support for the elevated basal inflammation (dysfunction) of both subcutaneous and visceral fat depots of *APOE2* mice, and the condition was further exaggerated when fed the Western-type diet.

Elevated adipose tissue macrophage content and inflammation in *APOE2* mice. To further test the hypothesis that adipose tissues in *APOE2* mice are dysfunctional (more inflamed), macrophage recruitment and retention marker gene expression in both subcutaneous (inguinal) and visceral (gonadal) adipose depots were compared between basal and Western diet–fed *APOE2* and *APOE3* mice. In subcutaneous adipose tissues, no significant differences in expression of monocyte chemoattractant protein-1 (MCP-1) and MIP-1α were observed between *APOE2* and *APOE3* mice under basal dietary conditions, with elevated MIP-1α expression observed in *APOE2* mice after feeding the Western-type diet for 4 weeks (Fig. 6*C* and *D*). Interestingly, the number of macrophages, as measured by F4/80 mRNA, was significantly higher (by approximately twofold) in subcutaneous adipose of *APOE2* mice compared with *APOE3* mice (Fig.

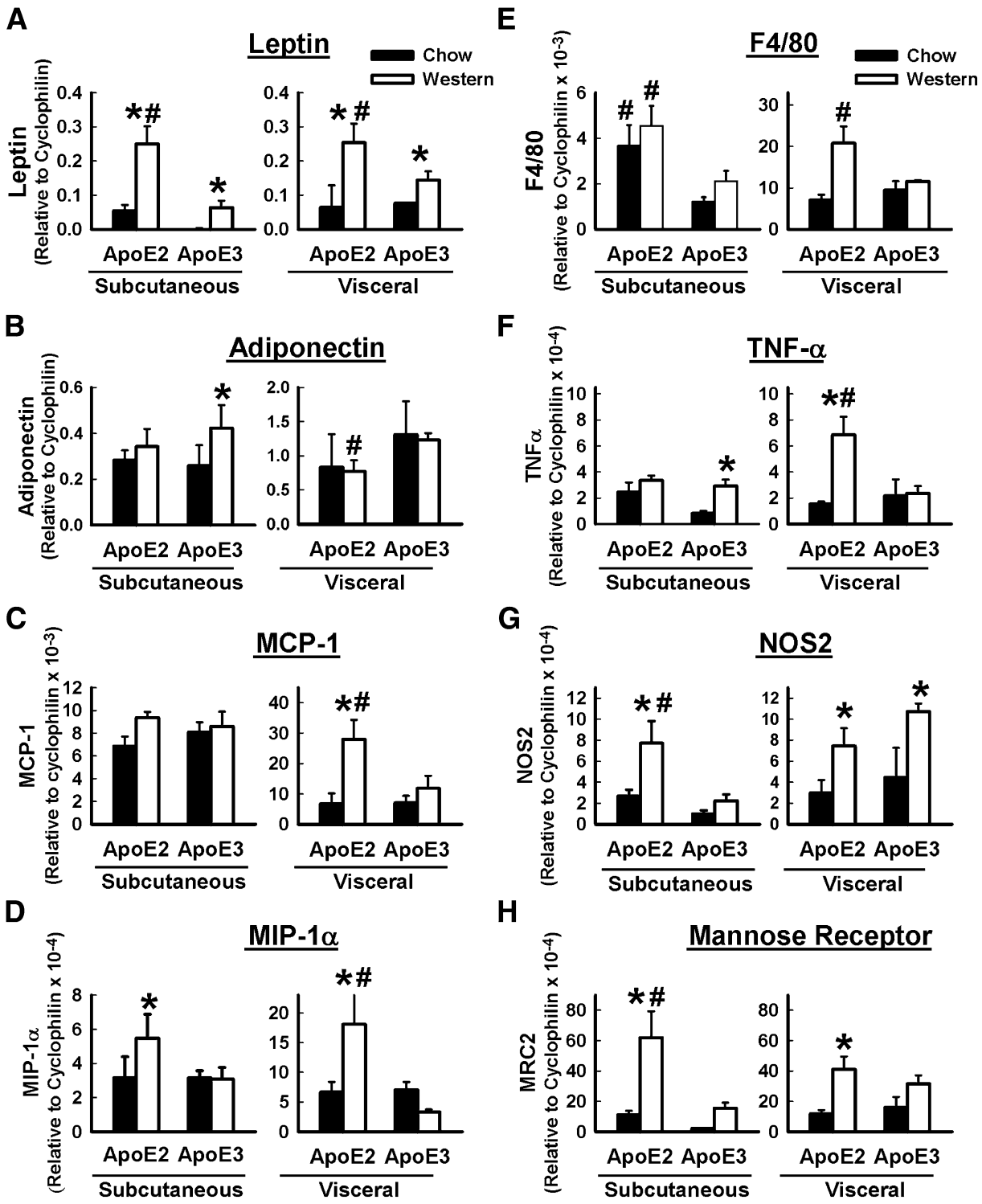

FIG. 6. Gene expression in adipose tissues. Total mRNA was isolated from subcutaneous and visceral adipose tissues of chow- (filled bars) and Western diet–fed (open bars) *APOE2* and *APOE3* mice and used for quantification by qPCR. Gene expression levels were normalized to levels of cyclophilin gene expression. *A*: Leptin expression levels. *B*: Adiponectin expression levels. *C*: MCP-1 expression levels. *D*: MIP-1α expression levels. *E*: Macrophage marker gene F4/80 expression levels. *F*: TNF-α expression levels. *G*: Inducible NOS2 expression levels. *H*: MRC2 expression levels. The data were reported as mean ± SD from six mice in each group. *$P < 0.05$, difference from mice with the same genotype fed chow diet; #$P < 0.05$, difference from mice with different genotype fed the same diet.

6*E*), indicating elevated basal inflammation even in subcutaneous adipose of *APOE2* mice. The influence of *APOE2* on diet-induced adipose tissue inflammation was readily observed in visceral adipose tissues, with MCP-1, MIP-1α, and F4/80 gene expression elevated three- to fourfold in *APOE2* mice, whereas expression of these genes was not significantly different in *APOE3* mice after 4 weeks on Western diet (Fig. 6*C*–*E*). The elevated expression of F4/80 genes in adipose tissues of *APOE2* mice compared with *APOE3* mice was consistent with a similar

increase of F4/80$^+$ cells in the stromal-vascular cell fractions of *APOE2* adipose tissues observed by flow cytometry (*APOE2* mice, 47.54% macrophages; *APOE3* mice, 33.68% macrophages; $P < 0.05$).

The expression of proinflammatory M1 macrophage marker genes, such as tumor necrosis factor-α (TNF-α) and NOS2 (32), was also significantly elevated in subcutaneous adipose tissues of *APOE2* mice compared with *APOE3* mice under both basal and Western diet conditions. In fact, the expression of both TNF-α and NOS2 in chow-fed *APOE2* mice was similar to that observed in Western diet–fed *APOE3* mice (Fig. 6*F* and *G*). Western diet feeding further exaggerated the elevated expression of NOS2 in subcutaneous adipose tissues of *APOE2* mice (Fig. 6*G*). Likewise, in the more inflammatory visceral adipose tissues, TNF-α expression was similar between basal diet–fed *APOE2* mice and *APOE3* mice fed either diet. The expression of TNF-α in visceral fat depots of *APOE2* mice, but not *APOE3* mice, was additionally increased after feeding the Western diet for 4 weeks (Fig. 6*F*). The expression of NOS2 in visceral depots was similar and diet responsive in both *APOE2* and *APOE3* mice (Fig. 6*G*). Surprisingly, the expression levels of alternative macrophage activation genes, such as the type 2 mannose receptor (MRC2) (31), were also significantly higher in subcutaneous adipose tissues of basal diet–fed *APOE2* mice, to a level similar to that observed in *APOE3* mice after Western diet feeding. Western diet further exaggerated alternative macrophage activation in subcutaneous adipose tissues of *APOE2* mice (Fig. 6*H*). In the typically more inflamed visceral adipose depots, no significant differences in MRC2 expression were observed between basal chow–fed *APOE2* and *APOE3* mice, and both strains responded to Western diet feeding with similar induction of MRC2 (Fig. 6*H*). Similar results were obtained using arginase-1 mRNA as a marker of M2 macrophages (data not shown). Taken together, these results indicate that macrophages in subcutaneous adipose tissues of *APOE2* mice are more activated compared with *APOE3* mice through both classical and alternative activation pathways, whereas both strains are sensitive to diet-induced activation of visceral adipose tissue macrophages.

Elevated plasma cytokine levels in *APOE2* mice. In addition to differences in gene expression between adipose tissues isolated from *APOE2* and *APOE3* mice, we also measured plasma levels of adipokines and inflammatory cytokines in these animals. Consistent with the gene expression data, no difference in plasma adiponectin levels was observed between *APOE2* and *APOE3* mice (Fig. 7*A*). In contrast, significantly higher levels of leptin, interleukin-6, and plasminogen activator inhibitor-1 were observed in the plasma of *APOE2* mice (Fig. 7*B–D*).

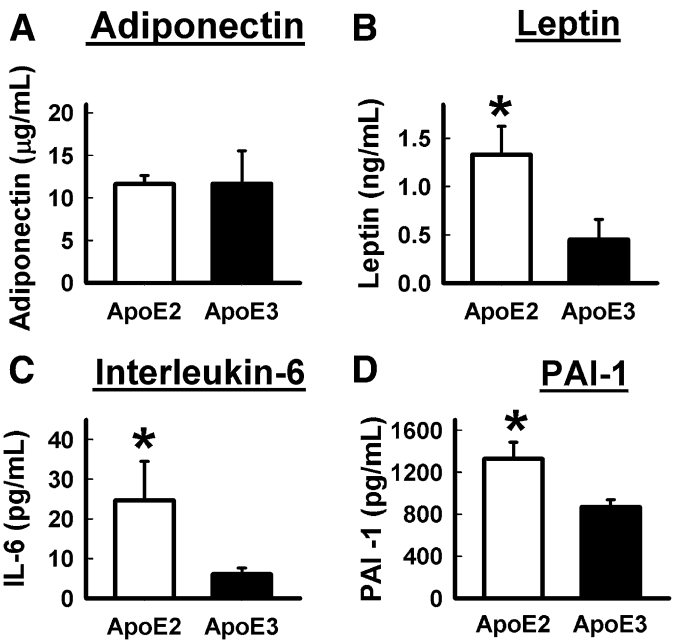

FIG. 7. Plasma cytokine levels. Plasma was obtained from *APOE2* (open bars) and *APOE3* (filled bars) to determine the levels of adiponectin (*A*), leptin (*B*), interleukin-6 (*C*), and plasminogen activator inhibitor-1 (PAI-1) (*D*). The data represent mean ± SD from six mice in each group. *$P < 0.05$, significant difference from *APOE3* mice.

DISCUSSION

Human population studies have suggested that the apoE2-encoding ε2 allele may be a genetic modifier for increased risk of developing obesity and type 2 diabetes (4,9,10). The current study used human *APOE2* and *APOE3* gene replacement mice and showed that the underlying mechanism is the impaired clearance of apoE2-containing triglyceride-rich lipoproteins from circulation, leading to increased postprandial lipid uptake by leukocytes to promote inflammation, and chronic lipid deposition in adipose tissues to increase adiposity and susceptibility to diet-induced obesity. The combination of elevated adiposity and inflammation accelerates adipose tissue dysfunction, with increased macrophage infiltration and inflammation observed in adipose tissues of *APOE2* mice after a short 4-week dietary regimen. The consequence of these metabolic changes is the accelerated hyperinsulinemia observed in Western diet–fed *APOE2* mice compared with *APOE3* mice.

The mechanism by which apoE2 promotes postprandial lipid uptake by leukocytes and chronic lipid deposition in adipose tissues has not been established. Typically, lipids from triglyceride-rich lipoproteins are taken up by leukocytes and adipocytes through two distinct mechanisms, one involving lipoprotein lipase–mediated hydrolysis of the triglycerides followed by the uptake of the liberated fatty acids (33,34) and another via whole lipoprotein particle endocytosis after binding to LDL receptor–related protein-1 (LRP1), VLDL receptor, and/or heparin sulfate proteoglycans (HSPGs) (27,35,36). Previous studies have shown that apoE2-containing lipoproteins are poor substrates for lipoprotein lipase in comparison with apoE3 lipoproteins (37). Moreover, lipoprotein lipase expression was reported to be similar between *APOE2* and *APOE3* mice, but the *APOE2* adipocytes are defective in the uptake of lipase-derived fatty acids (38). Importantly, despite the defective binding of apoE2 lipoproteins to the LDL receptor, apoE2 lipoproteins bind with similar affinity as apoE3 lipoproteins to LRP1, VLDL receptor, and HSPG (39–43). Previous studies have shown the importance of LRP1, VLDL receptor, and HSPG in mediating lipid deposition in adipocytes (27,35,36). The receptor-associated protein, which binds to both LRP1 and VLDL receptor in inhibiting their interaction with apoE-containing lipoproteins, has also been reported to suppress triglyceride-rich lipoprotein-induced leukocyte activation (19). Thus, it appears more likely that the elevated postprandial leukocyte lipid uptake and inflammation as well as the chronic

dietary lipid deposition in *APOE2* mice are mediated through apoE2-containing triglyceride-rich lipoprotein endocytosis via one of the cell surface receptors. Nevertheless, additional studies are necessary to test this hypothesis.

It is interesting to note that *APOE2* adipocytes were previously reported to have an increased rate of stored triglyceride hydrolysis as well as impaired de novo lipogenesis compared with *APOE3* adipocytes (38). Despite these abnormalities, we observed elevated obesity with increased adipocyte cell size in *APOE2* mice compared with *APOE3* mice upon chronic feeding of the Western-type diet. These observations illustrated that the impaired hepatic clearance of apoE2-containing triglyceride-rich lipoproteins leads to redistribution of dietary fat to adipocytes in *APOE2* mice to promote obesity. Moreover, the elevated hydrolysis and turnover of stored triglycerides is also expected to promote adipocyte lipotoxicity to exacerbate inflammation (44). The observation of an increased number of crown-like structures, representing macrophage aggregates surrounding dead adipocytes (29), in *APOE2* adipose tissues compared with *APOE3* adipose tissues is consistent with this interpretation.

In summary, our data showed increased sensitivity to postprandial inflammation and diet-induced obesity in mice expressing human apoE2 compared with apoE3. It is important to note that, in contrast to human ε2 carriers, the *APOE2* mice displayed hyperlipidemia even under low-fat, chow-fed conditions. There are also significant differences in triglyceride-rich lipoprotein metabolism between mice and humans. Determining whether human ε2 carriers are also more sensitive to postprandial inflammation and diet-induced obesity compared with ε3 subjects will require additional studies.

ACKNOWLEDGMENTS

This study was supported by a grant from the National Institutes of Health (DK-074932).

No potential conflicts of interest relevant to this article were reported.

D.G.K. conducted the experiments, analyzed the data, and wrote the manuscript. E.S.K., J.E.B., C.M., and C.T.G. conducted the experiments and analyzed the data. T.K.C. and N.L.W. analyzed the data, provided critical insights, and contributed to writing, reviewing, and editing the manuscript. D.Y.H. planned the project, designed the experiments, analyzed the data, and wrote and reviewed the manuscript. D.Y.H. is the guarantor of this work and, as such, had full access to all the data in the study and takes responsibility for the integrity of the data and the accuracy of the data analysis.

Parts of this study were presented in poster form at the 2011 Scientific Sessions of the American Heart Association, Orlando, Florida, 12–16 November 2011.

REFERENCES

1. Mahley RW, Weisgraber KH, Huang Y. Apolipoprotein E: structure determines function, from atherosclerosis to Alzheimer's disease to AIDS. J Lipid Res 2009;50(Suppl.):S183–S188
2. Getz GS, Reardon CA. Apoprotein E as a lipid transport and signaling protein in the blood, liver, and artery wall. J Lipid Res 2009;50(Suppl.):S156–S161
3. Eto M, Watanabe K, Ishii K. Reciprocal effects of apolipoprotein E alleles (epsilon 2 and epsilon 4) on plasma lipid levels in normolipidemic subjects. Clin Genet 1986;29:477–484
4. Duman BS, Oztürk M, Yilmazer S, Hatemi H. Apolipoprotein E polymorphism in Turkish subjects with type 2 diabetes mellitus: allele frequency and relation to serum lipid concentrations. Diabetes Nutr Metab 2004;17:267–274
5. Zeggini E, Weedon MN, Lindgren CM, et al.; Wellcome Trust Case Control Consortium (WTCCC). Replication of genome-wide association signals in UK samples reveals risk loci for type 2 diabetes. Science 2007;316:1336–1341
6. Scott LJ, Mohlke KL, Bonnycastle LL, et al. A genome-wide association study of type 2 diabetes in Finns detects multiple susceptibility variants. Science 2007;316:1341–1345
7. Saxena R, Voight BF, Lyssenko V, et al.; Diabetes Genetics Initiative of Broad Institute of Harvard and MIT, Lund University, and Novartis Institutes of BioMedical Research. Genome-wide association analysis identifies loci for type 2 diabetes and triglyceride levels. Science 2007;316:1331–1336
8. Zeggini E, Scott LJ, Saxena R, et al.; Wellcome Trust Case Control Consortium. Meta-analysis of genome-wide association data and large-scale replication identifies additional susceptibility loci for type 2 diabetes. Nat Genet 2008;40:638–645
9. Zeljko HM, Škarić-Jurić T, Narančić NS, et al. E2 allele of the apolipoprotein E gene polymorphism is predictive for obesity status in Roma minority population of Croatia. Lipids Health Dis 2011;10:9
10. Anthopoulos PG, Hamodrakas SJ, Bagos PG. Apolipoprotein E polymorphisms and type 2 diabetes: a meta-analysis of 30 studies including 5423 cases and 8197 controls. Mol Genet Metab 2010;100:283–291
11. Kalix B, Meynet MC, Garin MC, James RW. The apolipoprotein ε2 allele and the severity of coronary artery disease in type 2 diabetic patients. Diabet Med 2001;18:445–450
12. Vaisi-Raygani A, Rahimi Z, Nomani H, Tavilani H, Pourmotabbed T. The presence of apolipoprotein ε4 and ε2 alleles augments the risk of coronary artery disease in type 2 diabetic patients. Clin Biochem 2007;40:1150–1156
13. Oda H, Yorioka N, Ueda C, Kushihata S, Yamakido M. Apolipoprotein E polymorphism and renal disease. Kidney Int Suppl 1999;71:S25–S27
14. Couderc R, Mahieux F, Bailleul S, Fenelon G, Mary R, Fermanian J. Prevalence of apolipoprotein E phenotypes in ischemic cerebrovascular disease. A case-control study. Stroke 1993;24:661–664
15. Sentí M, Nogués X, Pedro-Botet J, Rubiés-Prat J, Vidal-Barraquer F. Lipoprotein profile in men with peripheral vascular disease. Role of intermediate density lipoproteins and apoprotein E phenotypes. Circulation 1992;85:30–36
16. de Andrade M, Thandi I, Brown S, Gotto A Jr, Patsch W, Boerwinkle E. Relationship of the apolipoprotein E polymorphism with carotid artery atherosclerosis. Am J Hum Genet 1995;56:1379–1390
17. Hui DY, Innerarity TL, Mahley RW. Defective hepatic lipoprotein receptor binding of β-very low density lipoproteins from type III hyperlipoproteinemic patients. Importance of apolipoprotein E. J Biol Chem 1984;259:860–869
18. Higgins LJ, Rutledge JC. Inflammation associated with the postprandial lipolysis of triglyceride-rich lipoproteins by lipoprotein lipase. Curr Atheroscler Rep 2009;11:199–205
19. Gower RM, Wu H, Foster GA, et al. CD11c/CD18 expression is upregulated on blood monocytes during hypertriglyceridemia and enhances adhesion to vascular cell adhesion molecule-1. Arterioscler Thromb Vasc Biol 2011;31:160–166
20. Alipour A, van Oostrom AJHHM, Izraeljan A, et al. Leukocyte activation by triglyceride-rich lipoproteins. Arterioscler Thromb Vasc Biol 2008;28:792–797
21. Ceriello A, Quagliaro L, Piconi L, et al. Effect of postprandial hypertriglyceridemia and hyperglycemia on circulating adhesion molecules and oxidative stress generation and the possible role of simvastatin treatment. Diabetes 2004;53:701–710
22. Harbis A, Perdreau S, Vincent-Baudry S, et al. Glycemic and insulinemic meal responses modulate postprandial hepatic and intestinal lipoprotein accumulation in obese, insulin-resistant subjects. Am J Clin Nutr 2004;80:896–902
23. Rivellese AA, Bozzetto L, Annuzzi G. Postprandial lipemia, diet, and cardiovascular risk. Curr Cardiovasc Risk Rep 2009;3:5–11
24. Sullivan PM, Mezdour H, Quarfordt SH, Maeda N. Type III hyperlipoproteinemia and spontaneous atherosclerosis in mice resulting from gene replacement of mouse Apoe with human Apoe*2. J Clin Invest 1998;102:130–135
25. Sullivan PM, Mezdour H, Aratani Y, et al. Targeted replacement of the mouse apolipoprotein E gene with the common human APOE3 allele enhances diet-induced hypercholesterolemia and atherosclerosis. J Biol Chem 1997;272:17972–17980
26. Hixson JE, Vernier DT. Restriction isotyping of human apolipoprotein E by gene amplification and cleavage with HhaI. J Lipid Res 1990;31:545–548
27. Hofmann SM, Zhou L, Perez-Tilve D, et al. Adipocyte LDL receptor-related protein-1 expression modulates postprandial lipid transport and glucose homeostasis in mice. J Clin Invest 2007;117:3271–3282

28. Hofmann SM, Perez-Tilve D, Greer TM, et al. Defective lipid delivery modulates glucose tolerance and metabolic response to diet in apolipoprotein E-deficient mice. Diabetes 2008;57:5–12
29. Cinti S, Mitchell G, Barbatelli G, et al. Adipocyte death defines macrophage localization and function in adipose tissue of obese mice and humans. J Lipid Res 2005;46:2347–2355
30. van Oostrom AJHHM, Sijmonsma TP, Verseyden C, et al. Postprandial recruitment of neutrophils may contribute to endothelial dysfunction. J Lipid Res 2003;44:576–583
31. Drechsler M, Megens RTA, van Zandvoort M, Weber C, Soehnlein O. Hyperlipidemia-triggered neutrophilia promotes early atherosclerosis. Circulation 2010;122:1837–1845
32. Olefsky JM, Glass CK. Macrophages, inflammation, and insulin resistance. Annu Rev Physiol 2010;72:219–246
33. den Hartigh LJ, Connolly-Rohrbach JE, Fore S, Huser TR, Rutledge JC. Fatty acids from very low-density lipoprotein lipolysis products induce lipid droplet accumulation in human monocytes. J Immunol 2010;184:3927–3936
34. Wang H, Eckel RH. Lipoprotein lipase: from gene to obesity. Am J Physiol Endocrinol Metab 2009;297:E271–E288
35. Goudriaan JR, Tacken PJ, Dahlmans VEH, et al. Protection from obesity in mice lacking the VLDL receptor. Arterioscler Thromb Vasc Biol 2001;21:1488–1493
36. Wilsie LC, Chanchani S, Navaratna D, Orlando RA. Cell surface heparan sulfate proteoglycans contribute to intracellular lipid accumulation in adipocytes. Lipids Health Dis 2005;4:2
37. Huang Y, Liu XQ, Rall SC Jr, Mahley RW. Apolipoprotein E2 reduces the low density lipoprotein level in transgenic mice by impairing lipoprotein lipase-mediated lipolysis of triglyceride-rich lipoproteins. J Biol Chem 1998;273:17483–17490
38. Huang ZH, Maeda N, Mazzone T. Expression of the human apoE2 isoform in adipocytes: altered cellular processing and impaired adipocyte lipogenesis. J Lipid Res 2011;52:1733–1741
39. Ruiz J, Kouiavskaia D, Migliorini M, et al. The apoE isoform binding properties of the VLDL receptor reveal marked differences from LRP and the LDL receptor. J Lipid Res 2005;46:1721–1731
40. Beisiegel U, Weber W, Ihrke G, Herz J, Stanley KK. The LDL-receptor-related protein, LRP, is an apolipoprotein E-binding protein. Nature 1989; 341:162–164
41. Takahashi S, Oida K, Ookubo M, et al. Very low density lipoprotein receptor binds apolipoprotein E2/2 as well as apolipoprotein E3/3. FEBS Lett 1996;386:197–200
42. Futamura M, Dhanasekaran P, Handa T, Phillips MC, Lund-Katz S, Saito H. Two-step mechanism of binding of apolipoprotein E to heparin: implications for the kinetics of apolipoprotein E-heparan sulfate proteoglycan complex formation on cell surfaces. J Biol Chem 2005;280:5414–5422
43. Ji ZS, Pitas RE, Mahley RW. Differential cellular accumulation/retention of apolipoprotein E mediated by cell surface heparan sulfate proteoglycans. Apolipoproteins E3 and E2 greater than e4. J Biol Chem 1998;273:13452–13460
44. Listenberger LL, Han X, Lewis SE, et al. Triglyceride accumulation protects against fatty acid-induced lipotoxicity. Proc Natl Acad Sci USA 2003; 100:3077–3082